Laser Physics, Vol. 11, No. 1, 2001, pp. 39–49.

Absorption Spectroscopy with Quantum Cascade Lasers

A. A. Kosterev*, R. F. Curl*, F. K. Tittel*, C. Gmachl, F. Capasso**, D. L. Sivco**, J. N. Baillargeon**, A. L. Hutchinson**, and A. Y. Cho****

** Rice Quantum Institute, Rice University, Houston, TX, 77251-1892 USA*

e-mail: akoster@rice.edu

*** Bell Laboratories, Lucent Technologies, 600 Mountain Avenue, Murray Hill, NJ, 07974 USA*

Received July 16, 2000

Abstract—Novel pulsed and cw quantum cascade distributed feedback (QC-DFB) lasers operating near λ = 8 μm were used for detection and quantification of trace gases in ambient air by means of sensitive absorption spectroscopy. N_2O, $^{12}CH_4$, $^{13}CH_4$, and different isotopic species of H_2O were detected. Also, a highly selective detection of ethanol vapor in air with a sensitivity of 125 parts per billion by volume (ppb) was demonstrated.

INTRODUCTION

Infrared laser absorption spectroscopy is an extremely effective tool for detecting trace gases. The demonstrated sensitivity of this technique is at the parts per billion (ppb) level. Presently, the usefulness of the laser spectroscopy approach is limited by the availability of convenient tunable sources in the spectroscopically important "fingerprint" region from 3 to 20 μm. The available options include cryogenically cooled lead salt diode lasers [1] and coherent sources based on difference frequency generation (DFG) [2]. Sensors based upon lead salt diode lasers are typically large in size and require consumables because the diodes operate at T < 90 K. DFG based sources (especially PPLN based) are shown to be very robust, but they generate inherently low IR power. We have demonstrated that DFG based sensors are suitable for many atmospheric monitoring applications. However, their spectral coverage is currently limited to wavelengths shorter than 5 μm by the optical transparency of suitable nonlinear optical crystals such as periodically poled $LiNbO_3$.

The recent development of quantum cascade lasers with distributed feedback (QC-DFB) fabricated by band structure engineering [3] offer an attractive option for IR absorption spectroscopy. Compared to Pb-salt diode lasers, QC-DFB lasers allow the realization of very compact narrow-linewidth mid-IR sources combining single-frequency operation and substantially higher powers (tens of mW) at mid-IR wavelengths (3.5 to 17 μm) (see Fig. 1). Pulsed DFB QC lasers are the only semiconductor lasers able to emit mid-IR radiation at room temperature (cw operation requires temperatures <150 K at this time). The higher power of QC lasers permits the use of advanced detection techniques that improve S/N ratio of trace gas spectra and decrease the apparatus size. For example in Cavity Enhanced Spectroscopy (CES) an effective absorption pathlength of hundreds of meters can be obtained in a laptop-size device [4, 5]. The large wavelength coverage available with QC lasers allows numerous molecular trace gas species to be monitored. Recent measurements with QC-DFB lasers have demonstrated the usefulness of these devices for sensitive highly selective real time trace gas concentration measurements based on absorption spectroscopy with sensitivities of several parts per billion (ppbv) [6–12].

In designing a QC laser based gas sensor, the first choice to be made is whether to operate the lasers in pulsed mode near room temperature or cw near liquid nitrogen temperature. Clearly room temperature operation is convenient in dispensing with cryogenic liquids and the need for an optical dewar. However, strong power dissipation in the active region limits the operation of quantum cascade lasers in such condition to pulses of several nanoseconds duration. The rapid changes of current that occur with short (nanoseconds) pulse excitation lead to frequency chirping and an increase in laser linewidth from less than 50 MHz for cw operation to >300 MHz. Room temperature pulsed operation also results in greatly reduced duty cycle. Thus cw operation of a QC-DFB at cryogenic temperatures is still advantageous for many applications, especially if a compact liquid nitrogen dewar is employed. In our work, we describe design and performance of two gas sensors, one based on a quasi-cw (long pulses) driven laser at cryogenic temperature, and another one based on the laser at near-room temperature driven by nanosecond-long current pulses.

DETECTION OF TRACE GASES WITH A QUASI-CW QC-DFB LASER

Type-I quantum cascade lasers (presently the only kind of QC lasers capable of single-frequency mid-IR operation) dissipate as much as 10 W in cw operation. The high power dissipation is more than compensated

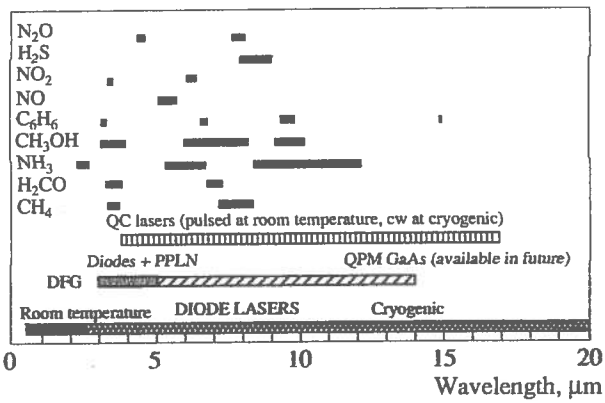

Fig. 1. Frequency coverage by different compact narrow-line sources.

by a high conversion efficiency giving up to 450 mW. However, the power consumption causes fast boil off of liquid nitrogen and frequency drift, which restricts data acquisition times. We have found that a convenient way to avoid these effects is to operate the laser in a quasi-cw mode supplying current in pulses of 120 to 235 μs duration at a 800 to 1000 Hz repetition rate. This somewhat reduces the duty cycle, but does not adversely affect the frequency resolution. From each pulse a frequency scan of up to 2 cm^{-1} is produced and a number of such scans are averaged.

The schematic of a cw QC-DFB laser based gas sensor is shown in Fig. 2. Laser current was supplied in pulses of 120 to 235 μs duration at a 800 to 1000 Hz repetition rate by applying rectangular pulses to the external modulation input of a low-noise driver. When a rectangular pulse is applied to the external modulation input, the laser current experiences a 40 μs delayed jump from zero to some intermediate value, and then grows exponentially to a steady-state level, which permits fast current scanning of the QC-DFB laser frequency using a pulse generator. The use of a pulse generator instead of a function generator enabled easy variation of the laser duty cycle and thus its average operating temperature and laser frequency. The resulting nonlinear frequency-time dependence is perfectly reproducible and the nonlinearity is easily removed by data processing. This dependence is depicted in Fig. 3 as measured using the etalon fringes from two uncoated ZnSe surfaces inserted in the laser beam. Each current pulse resulted in a frequency scan covering ~2 cm^{-1}.

To suppress the influence of interfering effects, a "zero-air" background subtraction technique [1] was used. Spectra of ambient air and a pollutant-free zero air were alternatively taken. Replacing the air in the 3.3 l multipass cell required ~30 s. The zero-air signal (as a function of a datapoint number) was subtracted from the ambient air signal, normalized to the zero-air signal, and resulted in an absorption spectrum. In most of the measurements, pure air with an addition of 5% CO_2 was used as a zero gas. The resulting weak "negative absorption" CO_2 lines in the acquired spectra aided to the spectral calibration of wavelength scans.

A typical absorption spectrum of ambient air is shown in Fig. 4 as obtained with a QC-DFB laser using the setup shown in Fig. 2 and the procedure described above. Four strong methane lines, two strong nitrous oxide lines and several water lines corresponding to different isotopic species fall into the spectral range covered by this frequency scan. The spectrum depicted is the result of averaging over 6000 individual scans for both ambient air and zero-air. The acquisition and averaging of 6000 200 μs-long scans with 50 megasamples per second at 1 kHz repetition rate required approximately 30 seconds. Optimized software will permit faster data acquisition by utilizing a larger fraction of the current pulses.

The CH_4 and N_2O concentration levels in the ambient air were determined by fitting the envelopes of the stronger absorption lines with a Voigt function. The area under a fitting curve was compared with that predicted from the HITRAN database.

The accuracy of these measurements is limited by the slow variations of the baseline, which may contribute to the pressure-broadened spectral line wings. To estimate the minimum detectable absorbance, we have used the same technique as reported in our earlier work [8]. This consisted of selecting a part of the spectrum containing no absorption lines and setting the fitting procedure parameters to find an absorption feature similar to a CH_4 absorption line. The typical peak absorbance of such a feature did not exceed $\pm 3.5 \times 10^{-5}$, or 8×10^{-5} fractional absorption. For the strongest absorption lines in these experiments, a detection limit of 2.5 ppb for CH_4, 1.0 ppb for N_2O and 60 ppb for H_2O (absorption line at 1260.344 cm^{-1}) is estimated.

The spectral range near 8 μm is also useful for the detection of more complex organic molecules, such as ethanol (C_2H_5OH). The frequency of our QC-DFB laser falls close to the center of one of the absorption bands of this molecule. Figure 5 shows the ethanol vapor absorption spectra ((a) pure and (b) with the ambient air added to a pressure of 36.6 Torr) acquired with our QC-DFB laser in a 0.43 m long gas cell. The resolved spectral features clearly distinguish the ethanol absorption from other species. However, the high density of the pressure-broadened spectral lines makes the technique of individual line fitting with a Voigt profile inapplicable. Therefore another approach was used to find the ethanol concentration in the air. It is principally based on finding the correlation between previously acquired reference spectra and a spectrum of the sample under investigation (we shall call it a "test spectrum") under the same line-broadening conditions (same air pressure and temperature). For all data processing procedures described in the following sections, an ethanol absorption spectrum shown in Fig. 5b was

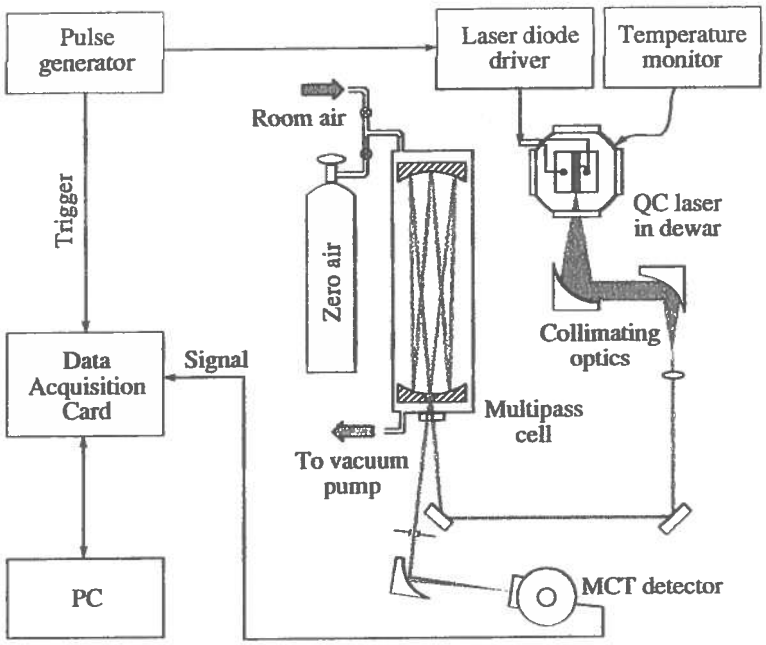

Fig. 2. Schematic of the cw QC-DFB laser based gas sensor.

used as a reference. The reference spectrum is of 2.87% ethanol vapor by volume in air, a total pressure of 36.6 Torr, pathlength of 0.43 m, and ranges from 1258.70 to 1260.24 cm^{-1}.

To increase the ethanol vapor concentration in the laboratory air, a few drops of ethanol were allowed to evaporate near the multipass cell air input as air flowed slowly, but continuously through the cell, and spectra were acquired 3, 7, 12 and 20 minutes later at the same 36.6 Torr air pressure in the multipass cell. The correlation approach was applied in two modifications: (a) using one-dimensional (1-D) linear regression to find a concentration of the ethanol vapor only, and (b) using multidimensional linear regression (MLR) to find concentrations of all known absorbing species in one fitting procedure.

As a first step of this analysis, a derivative of each spectral trace was calculated by subtracting a 9-datapoints-shifted array of data (3650 point total) from the original one. In our experiments, one datapoint step equals to a 4.2×10^{-4} cm^{-1} frequency change. This discrete derivation suppresses the influence of nearly constant background and the slow-changing wings of strong water lines. In a 1-D approach, each datapoint value from the test spectrum was plotted as a function of the corresponding datapoint value from the reference spectrum (Fig. 6). If only ethanol vapor absorbed the light in the test sample, and no measurement errors were present, all the points of this plot would lie on the straight line $y = kx$, where k is a ratio of ethanol absorbance in two samples. The absorption lines of CH_4, N_2O, and H_2O cause big "loops" strongly deviating from this linear law, and measurement errors lead to a scattering of data points. *Nevertheless, the large number of points ensures high* reliability of the linear fit slope value. Fitting was done in two steps. First, a linear fit was made using all the datapoints. Then, the points that are distant from the fit-

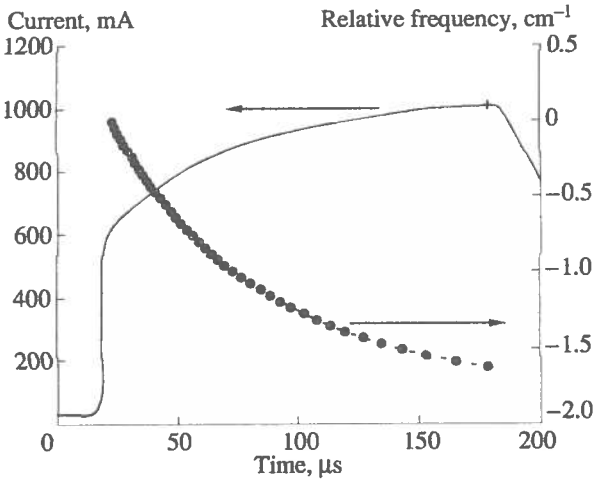

Fig. 3. Laser current and frequency as a function of time when a 200 μs long pulse is applied to the external modulation input of the laser current driver. Circles indicate positions of the etalon fringes. The fitting curve is a 4th order polynomial.

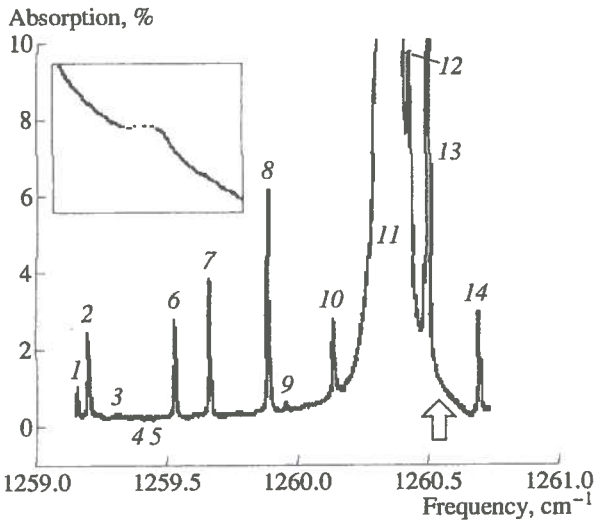

Fig. 4. An example of an absorption spectrum of room air obtained with a 100-m pathlength multipass cell and a zero-air background subtraction technique. The assignment of the strong spectral lines is shown: $H_2{}^{16}O$—*1*, *11*, *13*; N_2O—*2*, *3*, *10*; CH_4—*6*, *7*, *8*, *14*; $H_2{}^{18}O$—*9*; HDO—*12*; and CO_2 in the reference zero-air that appears as a negative absorption—*4*, *5*. A hollow arrow marks a position of the $^{13}CH_4$ absorption line shown on the inset.

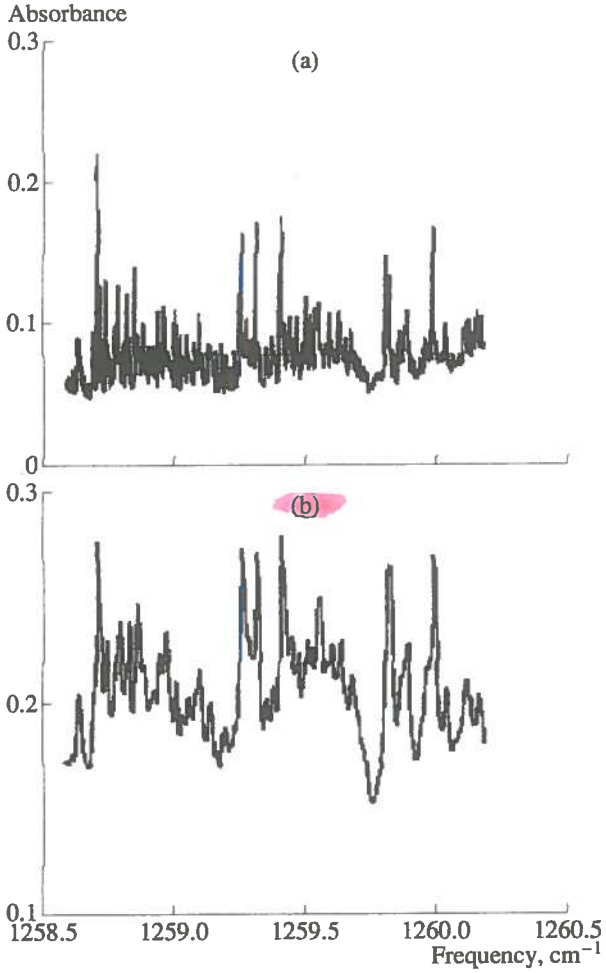

Fig. 5. Ethanol absorption spectra obtained in a 0.43 m long gas cell: (a) pure ethanol vapor at 1 Torr pressure; (b) same partial pressure of ethanol with room air added to a total pressure of 36.6 Torr.

ting line were considered as outliers and excluded from further consideration, and the remainder (~75% of the initial number) was re-fitted. In this way the influence of non-ethanol absorption lines was minimized. By determining that the slope for samples containing no ethanol fell within a range of $\pm 1 \times 10^{-3}$ about zero slope, it was possible to estimate the detection limit as 125 ppb on the basis that a slope of 1 is equal to $0.0287 \times (0.43\ \text{m}/100\ \text{m}) \approx 125$ ppm (reference cell ethanol concentration normalized to the ratio of the single-pass and multipass cell optical pathlengths).

Since the spectra of all the principal absorbing species (ethanol, methane, nitrous oxide and water) in the frequency range of the laser scan were separately available, a MLR analysis could be applied. Reference spectra of CH_4, N_2O, and H_2O were simulated using HITRAN data. The test spectrum was considered as a linear combination of four reference spectra of the absorbing species:

$$y_i = a_0 + \sum_{k=1}^{4} a_k x_{ki}, \qquad (1)$$

where y_i is the i-th datapoint of the test spectrum; a_k gives the contribution of each absorbing component to the resulting spectrum; k = 1–4 corresponds to C_2H_5OH, CH_4, N_2O, and H_2O, respectively; x_{ki} is the intensity of the k-th reference spectrum at the frequency of the i-th datapoint; a_0 represents an offset and should be close to zero, since derivatized spectra were used.

A multidimensional linear fit (MLR) to the dataset was performed using MathCad software in order to find a best-fitting 4-D hyperplane described by Eq. (1). Table 1 shows the results of the fitting procedure applied to the test spectra acquired 7 and 12 min after releasing ethanol. The offset a_0 was found negligibly small for all the datasets. The concentrations of all the components except for the ethanol remained practically the same within the measurement errors. The ethanol concentrations found using two different approaches to the analysis of data (1-D regression and MLR) are practically the same for the sample 2. Some discrepancy for the sample 1 is probably caused by the influence of non-ethanol lines on the 1-D linear regression. It should be noted that the relative error for the

CH_4, N_2O, and H_2O concentration is higher than that for the ethanol because of the smaller number of points involved, and also because of small shifts of line positions for the test and simulated reference spectra.

PULSED QC-DFB LASER BASED TRACE GAS DETECTION

A schematic of the pulsed QC-DFB laser based gas sensor configuration is shown in Fig. 7. A QC-DFB laser designed for pulsed near-room temperature operation at ~8 μm was mounted on a three-stage thermoelectric cooling module inside a compact evacuated housing shown in Fig. 8 ($75 \times 75 \times 75$ mm^3). The thermoelectric cooling module was driven by a temperature controller (Wavelength Electronics LFI-3751) communicating with a laptop computer through a *RS232* serial communication port. The temperature of the QC-DFB laser could be varied from –40°C to above room temperature. In practice, the laser temperature was usually kept below +6°C because of a rapid decrease in laser power, an increase of threshold current and the appearance of mode instabilities at higher temperatures. The optical configuration of this sensor was very similar to that used for cw QC laser based trace gas detection. The detector signal was measured using a gated integrator (Stanford Research Systems SR-250) and a 12-bit data acquisition card (DAQC) (National Instruments DAQCard-1200) with a laptop computer. An integration window of 15 ns was set to integrate the signal at the peak of ~35 ns FWHM detector response. The useful signal was separated in time from any interfering scattered light due to a 330 ns delay of the laser pulse in the multipass cell.

Short current pulses (~5 ns FWHM) were supplied to the laser through a low-impedance stripline. The pulse repetition rate was limited to 20 kHz by the minimum acquisition time of the gated integrator. A variable pedestal of computer-controlled sub-threshold current was added to each pulse, enabling "fast" wavelength tuning. A similar frequency scanning technique with an analogue sub-threshold linear current ramp was described in [11, 12]. In our experiments the current offset was created by applying an amplified computer-synthesized voltage from the D/A converter of the DAQC to the laser through a decoupling resistor $R_1 = 50\ \Omega$. Computer control adds flexibility to the device architecture, enabling arbitrary waveforms to be applied. We found that when the sub-threshold current exceeded 230 mA, the laser operation became unstable. This effect limited fast laser tunability to ~0.23 cm^{-1}. Slow laser frequency tuning was performed by changing the laser temperature. Variation of the laser temperature from –25 to +5°C allowed tuning in a spectral range from ~1255.5 to 1258.0 cm^{-1}. Frequency calibration curves for slow and fast laser scans are shown in Figs. 9a and 9b, respectively. These data are obtained using the interference fringes produced by two air-separated uncoated ZnSe surfaces. The slow scan is linear with a coefficient of –0.084 cm^{-1}/°C. The solid line in Fig. 9b shows a third order polynomial fit.

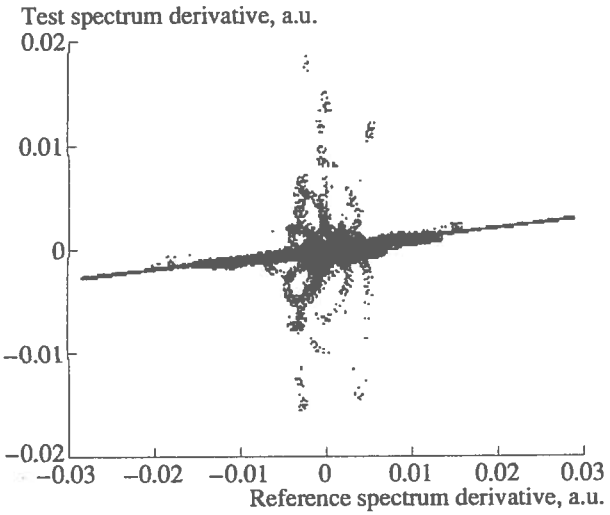

Fig. 6. Value of a test sample spectrum derivative as a function of the reference spectrum derivative. The test sample of room air is taken 7 minutes after evaporating a few drops of ethanol near the multipass cell. The fitting line slope yields *a value of* $k = 9.82 \times 10^{-2}$, *corresponding to an ethanol concentration of* 12.1 ppm.

Table 1. The concentration value of trace gas species in the air samples resulted from two different data analysis approaches. Samples 1 and 2 are taken 7 and 12 minutes after releasing the ethanol, respectively

Species	Measured concentration—sample 1		Measured concentration—sample 2	
	MLR	1-D regression	MLR	1-D regression
C_2H_5OH	11.60×10^{-6}	12.12×10^{-6}	1.44×10^{-6}	1.41×10^{-6}
CH_4	1.72×10^{-6}	–	1.70×10^{-6}	–
N_2O	0.302×10^{-6}	–	0.301×10^{-6}	–
H_2O	1.72×10^{-3}	–	1.73×10^{-3}	–

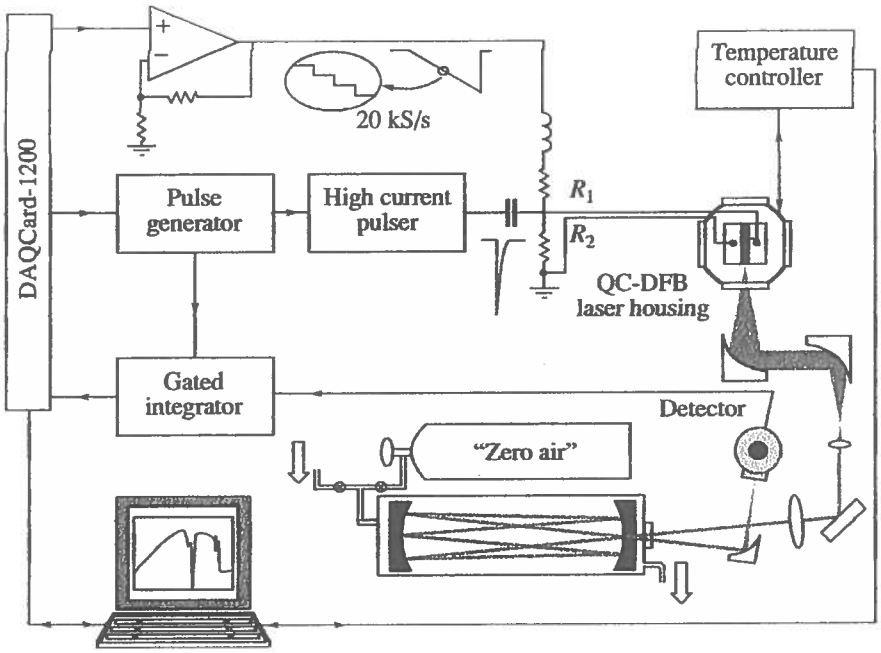

Fig. 7. Experimental arrangement for absorption spectroscopy with a pulsed QC-DFB laser. The laser is mounted on a thermoelectric cooler in an evacuated housing.

A compact pulser module with a fixed pulse duration of ~5 ns was used in the present laser spectrometer design to minimize the heating-related laser frequency chirp. It was connected to the laser with a high-frequency low-impedance stripline. A coupling resistor $R_2 = 7.9\ \Omega$ was connected to the stripline in order to suppress electrical oscillations in the circuit. The correct choice of R_2 is critical for the spectral properties of the QC-DFB laser radiation. The use of this resistor was found to ensure a significantly smaller laser linewidth (2×) at the same or even higher laser power levels.

In a fast-scan data acquisition mode, the laser temperature was first chosen so that the laser operated near an absorption line of interest. The pulse generator was triggered by the DAQC, and a computer-synthesized voltage pedestal was applied to each short high-current pump pulse. The intensity of each laser pulse was individually measured after the multipass cell, digitized and stored in the computer memory. Each scan consisted of 512 data points. The scans were repeated continuously and the data were averaged until a pre-set number of scans is reached.

The laser frequency exhibits an essentially nonlinear dependence on the offset voltage applied to the stripline as seen from Fig. 9b. This nonlinearity was taken into account and the voltage waveform was corrected so as to make the laser frequency vary linearly with the data point number during each scan.

To characterize the spectral properties of the laser pulses, the laser temperature was set to –8.5°C to enable a fast-scan across the CH_4 absorption line at 1256.601 cm^{-1}. The laser pulses were detected after passing through a 3 cm long cell that was alternatively filled with 1.25 Torr of CH_4 or evacuated. The measured absorption spectrum is shown in Fig. 10. From this spectrum we concluded that the laser lineshape is close to the Fourier-transform of a 3.1 ns long rectangular pulse on a broad pedestal that is due to the frequency chirping. The FWHM of the narrow spectral peak is 9.5×10^{-3} cm^{-1}, or 290 MHz. The laser lineshape thus acquired describes the instrument function of the laser spectrometer and was used in processing the absorption spectra described below.

This data acquisition technique was applied to detect CH_4 and N_2O in ambient air using a 100 m pathlength optical multipass cell. To enhance the accuracy of measurements, a "zero-air" subtraction technique was employed [1]. The laser temperature was set to –8.5°C to detect a CH_4 absorption line at 1256.601 cm^{-1}, and to –6.2°C to detect an N_2O absorption line at 1256.371 cm^{-1}. Examples of spectra acquired are shown in Fig. 11. The weaker line in Fig. 11a is due to HDO absorption at 1256.684 cm^{-1}. Both spectra were acquired at 85 Torr air pressure in the multipass cell. The baseline ("no absorption" line) of the acquired data exhibit some slow variations, despite the use of the zero-air technique. We attribute this to acoustic vibra-

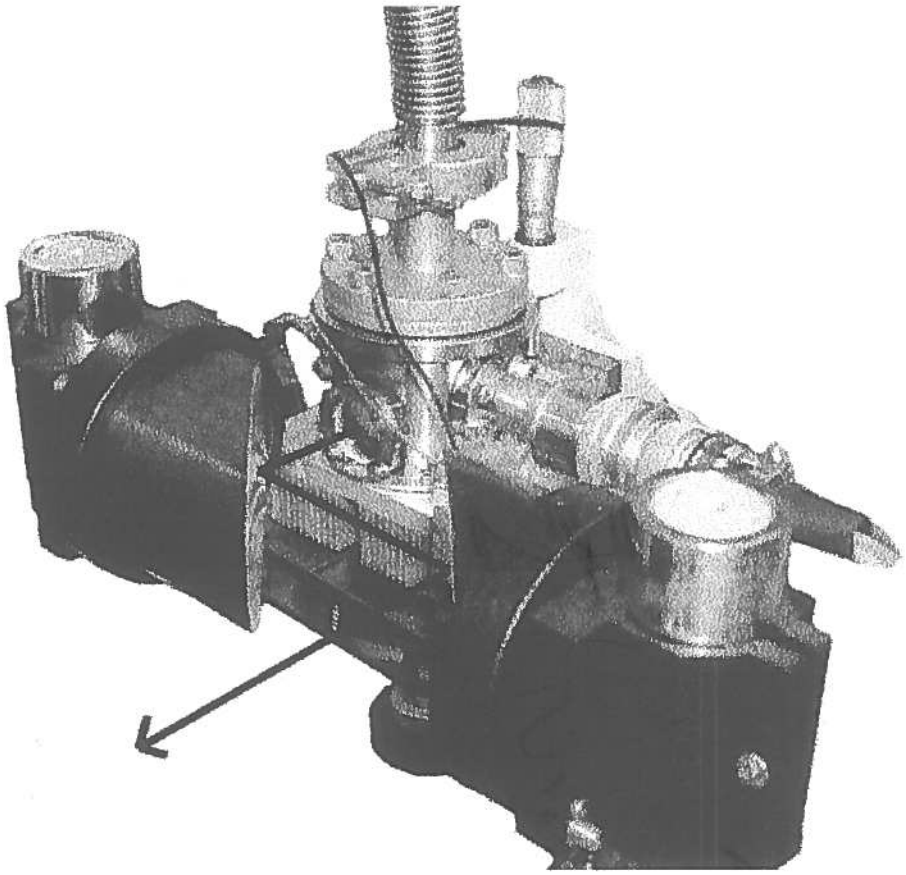

Fig. 8. The housing of a thermoelectrically cooled pulsed QC-DFB laser.

tions of the optical table that lead to small displacements of the laser beam. This was confirmed by a spectral analysis of the noise, which indicated a strong 90 Hz component correlating with optical table vibrations.

In order to determine the concentrations of absorbing species, the following procedure was applied:

1) The acquired spectra were numerically derivated by substracting a shifted array of the same data. This resulted in suppressing the baseline offset and slow baseline variations and gave a Dataset 1;

2) The absorption of air in the cell at 85 Torr was simulated using the HITRAN database, and this spectrum was convolved with the laser spectrometer instrument function shown in Fig. 10;

3) The resulting simulated absorption spectrum was numerically differentiated as in step (1) giving a Dataset 2;

Table 2. Measurements of trace gas concentrations by means of linear regression analysis of the fast scan data

	CH_4	HDO	N_2O
Concentration assumed in simulations, ppm	1.7	2.408	0.32
Simulated peak absorption	4.58%	0.29%	2.15%
Number of scans	1000	1000	200
Linear regression slope	1.195 ± 0.005	1.78 ± 0.05	0.998 ± 0.014
Resulting concentration, ppm	2.032 ± 0.009	4.28 ± 0.12	0.319 ± 0.004

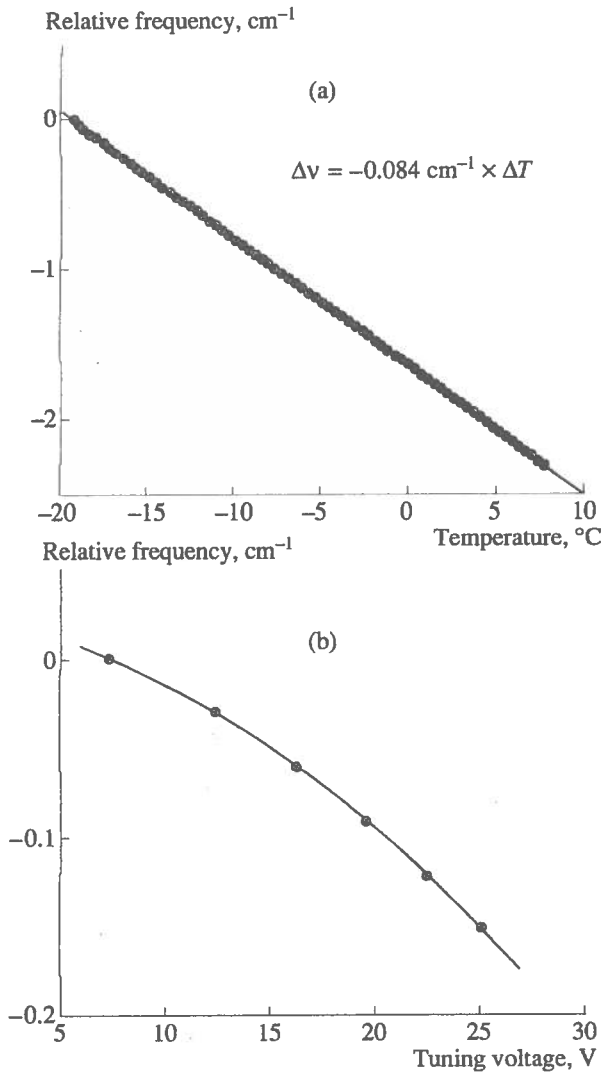

Fig. 9. Laser frequency: tuning (a) with temperature, (b) with a computer-controlled voltage applied to the resistor R_1 (shown in Fig. 1). The circles show positions of the etalon fringes used for calibration.

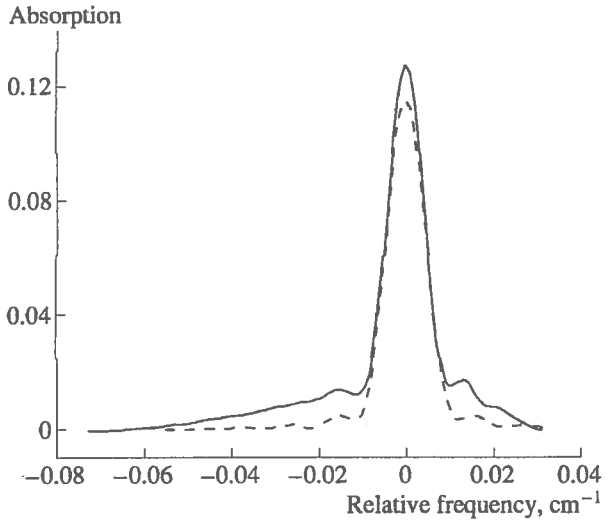

Fig. 10. The acquired envelope of the CH_4 absorption line at 1256.602 cm^{-1} (solid line), and the simulated envelope computed as a convolution of the Doppler-limited absorption line with a Fourier transform of a 3.1 ns long rectangular pulse (dashed line). The experimental data were obtained using a 3 cm long gas cell filled with 1.25 Torr of CH_4.

4) Each number of the Dataset 1 was plotted as a function of the corresponding number of the Dataset 2, and a linear regression analysis was applied to define the ratio of two absorption lines. This ratio was obtained as a slope of the linear fit.

This algorithm was applied to determine the concentrations of CH_4, HDO, and N_2O in air. The results are presented in Table 2. The methane concentration is in a good agreement with previous measurements in the Houston area [2]. Absorption of HDO, when compared to the HITRAN data, gives a relative humidity of 49%, which is lower than the hygrometer readings of 60%. However, the isotopic abundance of deuterium assumed in this database is 10 to 30% higher than in natural atmospheric water vapor, and this explains the deviation of the humidity calculated from the HDO absorption and the hygrometer readings. The concentration of N_2O was found to match the standard air value. The calculated standard deviation of the fitting line slope for all three absorption lines corresponds to a minimum detectable absorption of 3×10^{-4} when averaging over 200 scans (15 s) and 1.7×10^{-4} for 1000 scans.

In order to cover a larger frequency range in a single laser scan, slow temperature scanning is required. The simplest technique of acquiring such spectra consists of a slow continuous change of the laser temperature while periodically measuring the absorption of the laser pulses in the gas sample. When such measurements were carried out it was found that low-frequency noise is present in the acquired spectra with a peak-to-peak magnitude corresponding to ~1% absorption. This noise was mainly due to acoustic vibrations of the laboratory table (in particular, a strong 90 Hz component was found). To eliminate the low-frequency noise, we applied a modification of a wavelength-modulation technique. Our method is illustrated in Fig. 12. A sequence of 510 laser pulses with a repetition rate of 20 kHz was periodically generated, and pedestals of software-selectable voltages U_0, U_+, or U_- were added cyclically to each subsequent electrical excitation pulse. Such an alternating offset resulted in switching

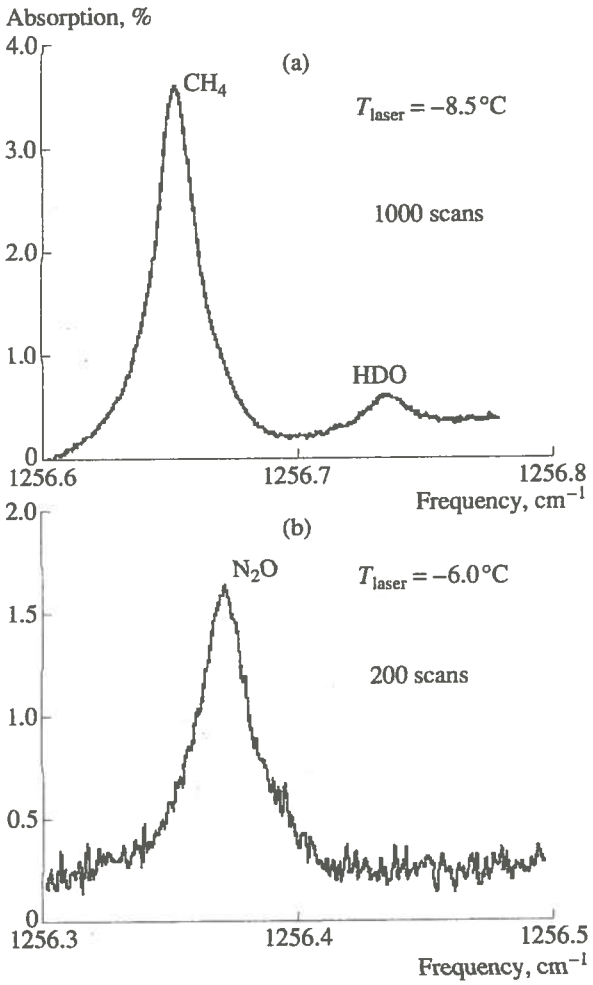

Fig. 11. Absorption spectra of ambient air in a 100 m pathlength multipass cell obtained with a fast frequency scanning technique: (a) laser temperature set to –8.5°C; (b) laser temperature set to –6.0°C. The pressure in the cell is 85 Torr.

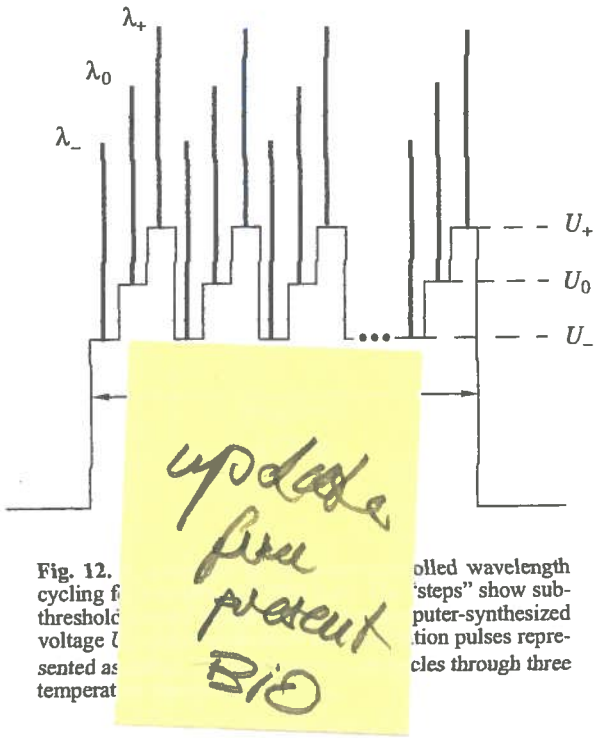

Fig. 12. cycling f threshold voltage U sented as temperat olled wavelength "steps" show sub- puter-synthesized tion pulses repre- cles through three

the laser wavelength between three (close) values, and the data were separately collected and averaged over 510/3 = 170 pulses for each wavelength. So, this 25.5 ms long train of 510 pulses resulted in almost simultaneous laser pulse attenuation measurements at three different temperature-dependent wavelengths. When repeated continuously, such measurements provide three arrays of data $S_0(T)$, $S_+(T)$, and $S_-(T)$ (Fig. 13a), where S is the IR detector signal. Differences $D(T) = S_+(T) - S_0(T)$ and $D^2(T) = S_+(T) + S_-(T) - 2S_0(T)$ yield discrete analogs of the first and the second derivatives $\partial S/\partial\nu$ and $\partial^2 S/\partial\nu^2$, respectively. Low-frequency noise adds the same fluctuations to all three data arrays, and therefore $D(T)$ and $D^2(T)$ are free of them. To obtain high $D(T)$ and $D^2(T)$ without a loss of resolution, the voltage pedestals were chosen so that the frequency differences $\nu_+ - \nu_0$ and $\nu_0 - \nu_-$ matched the halfwidth of an absorption feature, namely ~0.012 cm^{-1} at a pressure of 50 Torr.

An example of a $D^2(T)$ spectrum of ambient air is shown in Fig. 13b. This spectrum is derived from the set of data represented in Fig. 13a and was acquired at 50 Torr of air in the 100 m pathlength multipass cell. The $D^2(T)$ signal is not normalized to the laser intensity, which increases almost 8.5 times from +5 to –25°C. The noise did not depend noticeably on the temperature (and laser intensity) and also did not change when the laser beam was blocked. Separate measurements of the dark noise also revealed a match to the noise in a $D^2(T)$ signal. This confirms cancellation of the vibration-related fluctuations in the detected signal. It also means that the fluctuations in energy of the laser pulses are negligibly small compared to detection noise.

A comparison of the S/N ratio in the $D^2(T)$ data to the known absorption of CH_4, H_2O, and HDO lines near 1256.6 cm^{-1} (–7°C), showed that the detection limit of these measurements is 6×10^{-4} peak absorption. It compares to a minimum detectable absorption of 3×10^{-4} for 200 averaged fast scans. An estimate of the number of laser pulses N involved in the measurements of a single absorption line was made. An addition of uncorrelated fluctuations in quadrature when the derivative is calculated was also taken into account. This evaluation gave a four times lower N value for a slow scan than for a 200 times averaged fast scan. Hence, the detection limit normalized to $\sqrt{N}$ is the same for fast and slow

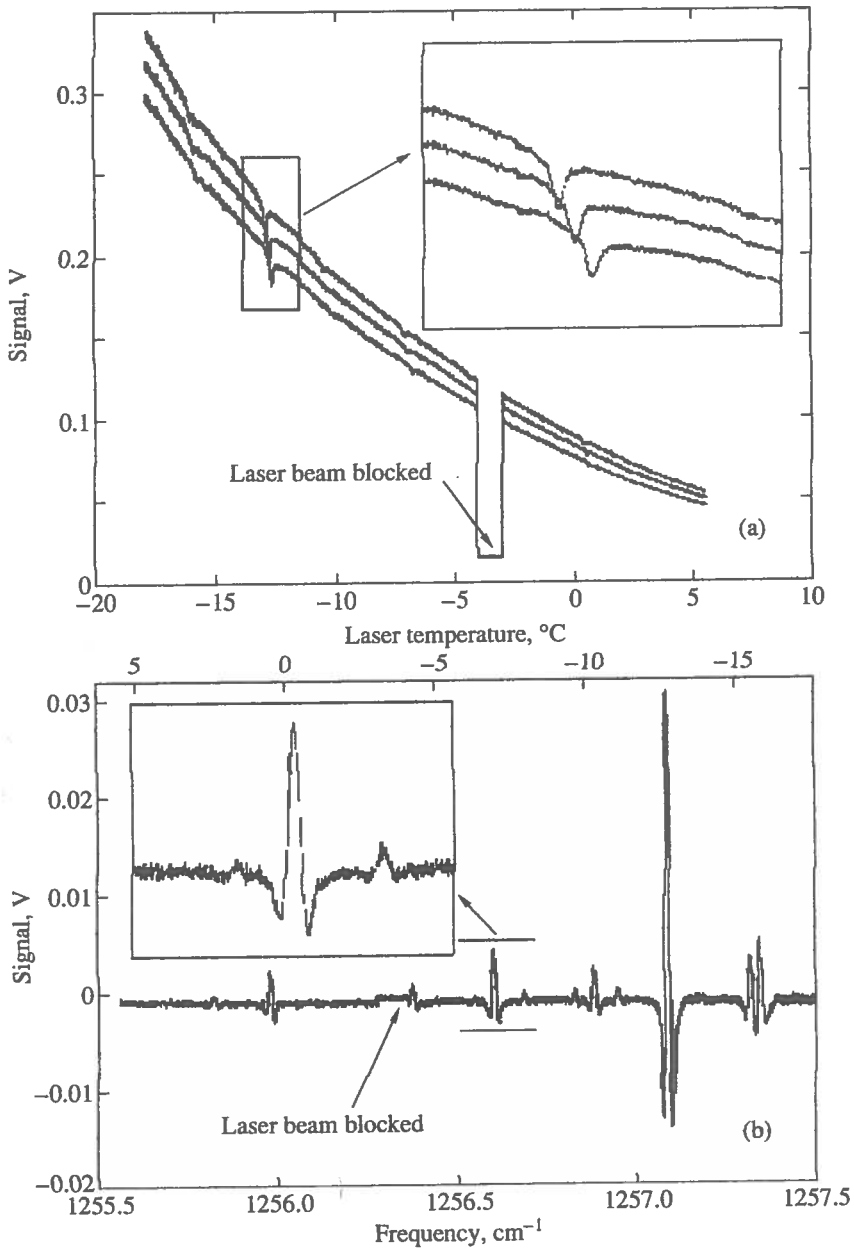

Fig. 13. Modified wavelength modulation spectroscopy: (a) IR detector signal simultaneously acquired at three laser wavelengths; (b) resulting second-derivative signal. Inset shows (left to right) weak H_2O, CH_4, and HDO absorption lines. Two lines to right on the main plot correspond to N_2O and HDO absorptions. The second-derivative signal is not normalized for changing laser power. The data are acquired at 50 Torr of air in the multipass cell.

scans. The sensitivity for both modes of spectral measurements is limited by random errors of the measuring electronics (mainly by detector dark noise).

CONCLUSION

Detection of trace gases in ambient air was demonstrated with both cw and pulsed QC DFB lasers. It was shown that near-room temperature operated pulsed QC-DFB lasers can be used for high-sensitivity detection of simple molecules when a spectral resolution of *~300 MHz is sufficient. A sensitivity of* 3.5×10^{-5} absorption was reached for the cw operated laser, and 1.7×10^{-4} for the pulsed QC-DFB laser based spectrometer. For detection of complex molecules with congested spectra the use of cryogenically cooled cw lasers